The autophilic anti-CD20 antibody DXL625 displays enhanced potency due to lipid raft-dependent induction of apoptosis

Marc G. Bingaman[a], Gargi D. Basu[a], Tiana C. Golding[a], Samuel K. Chong[a], Andrew J. Lassen[a], Thomas J. Kindt[a] and Christopher A. Lipinski[b]

Despite widespread use of anti-CD20 antibodies as therapeutic agents for oncologic and autoimmune indications, precise descriptions of killing mechanisms remain incomplete. Complement-dependent cytolysis and antibody-dependent cell-mediated cytotoxicity are indicated as modes of target cell depletion; however, the importance of apoptosis induction is controversial. Studies showing that the therapeutic anti-CD20 antibody rituximab (Rituxan) mediates apoptosis of tumor cell targets *in vitro* after cross-linking by anti-Fc reagents suggest that enhancement strategies applied to Fc-independent activities for anti-CD20 antibodies could improve therapeutic efficacy. An anti-CD20 antibody designated DXL625, with autophilic properties such as increased binding avidity, is shown here to independently induce caspase-mediated apoptosis of an established B-cell lymphoma line *in vitro*. Depletion of membrane cholesterol or chelation of extracellular calcium abrogated the pro-apoptotic activity of DXL625, indicating that intact lipid rafts and calcium are required for this activity. The Fc-mediated complement-dependent and antibody-dependent cellular killing mechanisms are maintained by DXL625 despite conjugation of the parental Rituxan antibody to the autophilic DXL peptide sequence. This study shows a strategy for improving anti-CD20 immunotherapy by endowing therapeutic antibodies with self-interacting properties. *Anti-Cancer Drugs* 21:532–542 © 2010 Wolters Kluwer Health | Lippincott Williams & Wilkins.

Anti-Cancer Drugs 2010, **21**:532–542

Keywords: apoptosis, CD20 receptor, DXL625, Rituxan

[a]InNexus Biotechnology Inc and [b]Mayo Clinic Arizona, Scottsdale, Arizona, USA

Correspondence to Dr Christopher A. Lipinski, MD, Mayo Clinic Arizona, 13400 East Shea Boulevard, Scottsdale, AZ 85259, USA
Tel: +1 480 342 1776; fax: +1 480 342 1744;
e-mail: Lipinski.christopher@mayo.edu

Received 15 December 2009 **Revised form accepted** 22 January 2010

Introduction

Therapeutic monoclonal antibodies have widespread applications in modern medicine and represent an area of growth for opportunities in the pharmaceutical industry [1,2]. Despite the myriad of candidate antibodies that have been generated over the past few decades, relatively few have proven to be safe and efficacious therapeutic agents [3,4]. In some cases, an approved therapeutic monoclonal antibody interacts with a molecular target playing a pivotal role in the pathobiology of a variety of diseases [5]. This affords the possibility of these proven agents to enter therapeutic areas beyond their original indications, expanding their utility and increasing their market value. Understanding the mechanism by which these biologic drugs function in the context of disease may suggest strategies for next-generation agents and expand the therapeutic application space.

Antibodies targeting the B-lymphocyte surface marker, CD20, have proven to be effective agents in the treatment of CD20-positive lymphoma and are remarkably well tolerated [6]. Prototypic of the anti-CD20 antibodies is rituximab (Rituxan; Genentech, USA), a highly used therapeutic monoclonal antibody for cancer treatment [6–9]. The pathobiological processes in which B-cells participate, however, extend beyond hematological malignancies and have led to additional indications for Rituxan such as rheumatoid arthritis [5,10]. Despite its success, information about precise mechanisms of action for Rituxan remains incomplete [11–15]. Available evidence strongly supports the role of Fc-dependent cytolytic activity, including complement-dependent cytotoxicity (CDC) and antibody-dependent cellular cytotoxicity (ADCC), in the mechanism of action for Rituxan [12,16–20]. Moreover, some have suggested that Rituxan has Fc-independent activities including proliferation inhibition and induction of apoptosis, although the latter is reported to require antibody cross-linking *in vitro* [21–27]. In addition, reduction in Fc-mediated activity resulting from Fc receptor polymorphisms on natural killer (NK) cells is presently believed to underlie some cases of Rituxan resistance in lymphoma [16,28–31]. It is likely that enhancement strategies applied to Fc-independent activities for anti-CD20 antibodies could improve therapeutic efficacy and reduce the need for patient exposure to more toxic, codministered chemotherapeutic agents.

Earlier work by Kohler *et al.* [32,33] showed that tumor cell targeting and killing by therapeutic antibodies was enhanced by coupling the antibody to a short, self-binding

0959-4973 © 2010 Wolters Kluwer Health | Lippincott Williams & Wilkins DOI: 10.1097/CAD.0b013e328337d485

peptide sequence, resulting in autophilic binding behavior (antibody–antibody interaction upon antigen–antibody engagement) while retaining antigenic specificity. This peptide sequence contained within residues 50–73 of the immunoglobulin heavy chain of the TEPC-15 murine anti-phosphorylcholine antibody (P01787), was identified based on its ability to specifically inhibit self-binding of autophilic murine antibodies [34,35]. The mechanism underlying potency enhancement yielded by engineering-in autophilic properties to nonautophilic antibodies has not been elucidated fully, but appears to involve potentiation of both Fc-dependent and Fc-independent functionalities.

This report describes the chimeric (mouse/human) anti-CD20 antibody, DXL625, created by the conjugation of a self-binding DXL sequence to Rituxan. DXL625 displays augmented in-vitro potency mediated by improved avidity compared with its parental antibody, shown here in the Ramos Burkitt's lymphoma cell line. A particular enhancement of Fc-independent cytolytic activity was seen for DXL625 through caspase-mediated apoptosis induction not observed in Rituxan. The induction of apoptosis by DXL625 is abrogated through the dissolution of lipid rafts and removal of extracellular Ca^{2+}. The Fc-dependent mechanisms, CDC and NK cell-mediated ADCC, both strongly induced by Rituxan, are fully maintained or even improved by DXL625.

Materials and methods

Synthesis of DXL625

DXL625 was manufactured at InNexus Biotechnology (Scottsdale, Arizona, USA) in a cGMP-like facility, by ultraviolet photo-conjugation of Rituxan to a self-binding ('autophilic') DXL peptide (WGAAASRNKANDYTTEYSASVKGRFIVSR) (Anaspec, San Jose, California, USA) through the N-terminal tryptophan moiety of the peptide, resulting in a majority of mono-conjugated ($\approx$65%) and a minority of di-conjugated ($\approx$10%) antibody as determined by liquid chromatography-mass spectrometry. DXL625 undergoes testing for sterility, stability, and being free of endotoxin contaminant, and is bottled at 10 mg/ml in a sodium citrate saline buffer (SCS) (25 mmol/l sodium citrate, 150 mmol/l NaCl, pH 6.5) and stored at 4°C before experimentation.

Antibodies and reagents

Rituxan was purchased from the Mayo Clinic Pharmacy (Scottsdale). CD20 peptide-mimetic (biotin-AHTPYINIYNCEPANPSEKNSPSTQYCY) was from Anaspec. Human peripheral blood lymphocytes (PBLs) were purified from healthy donor samples using standard Ficoll-Plaque separation. Normal human peripheral blood mononuclear cells (PBMCs) were from AllCells (Emeryville, California, USA). CD56-immunomagnetic separation beads and magnetic separation columns were from Miltenyi Biotec (Auburn, California, USA). Phycoerythrin (PE)-conjugated mouse anti-human CD19 was from Invitrogen (Carlsbad, California, USA). PE-conjugated mouse anti-human CD16 was from BD Biosciences (Franklin Lakes, New Jersey, USA). Rabbit anti-human CD20 (C-terminal) was from Epitomics (Burlingame, California, USA). Erythrolyse buffer (10X) was from AbD Serotec (Raleigh, North Carolina, USA). Fluorescein isothiocyanate (FITC)-conjugated goat anti-human IgG, calcein-AM, propidium iodide (PI), methyl-β-cyclodextrin (MβCD), RNase A, and rabbit HLA-ABC complement sera were from Sigma-Aldrich (St Louis, Missouri, USA). CellTiter-Glo and CaspACE kits were from Promega (Madison, Wisconsin, USA).

Binding assays

Surface plasmon resonance (SPR) was used to compare the rates of antibody binding to and dissociation from a CD20 peptide mimetic. CD20 peptides were bound to a streptavidin-coated sensor chip (GE Healthcare, Piscataway, New Jersey, USA) in order to achieve flow cells with varying antigen densities [100, 250, 1000 response units (RU)] as detected by the Biacore T100 device (GE Healthcare). Nonspecific interaction of antibodies was assessed by flowing Rituxan or DXL625 over streptavidin chips similarly coated with irrelevant peptides. In addition, the first of four flow cells remained uncoated and served as an in-experiment control for nonspecific association of antibody to the chip. Rituxan or DXL625 (15 μg/ml; 100 nmol/l) was injected for 120 s at 30 μl/min with 1X HBS-EP buffer (0.01 mol/l HEPES, 0.15 mol/l NaCl, 3 mmol/l EDTA, 0.05% (v/v) EDTA, pH 7.4) (association phase), followed for 60 s with 1X HBS-EP buffer only (dissociation phase), and regeneration for 30 s (10 mmol/l glycine, pH 2.5). The resulting change in RU was observed and plotted versus time.

Human PBLs were used in a Scatchard-type assay to compare the binding maximum (B_{max}) for Rituxan and DXL625 by flow cytometry. Eight-fold dilutions (0–300 μg/ml) of either Rituxan or DXL625 were incubated in whole healthy-donor peripheral blood for 20 min on ice followed by hypoosmotic lysis (1X Erythrolyse buffer). Remaining mononuclear lymphocytes were washed and CD20-bound antibodies were detected using FITC-conjugated goat anti-mouse IgG. Samples were acquired with the BD FACSCanto II (BD Biosciences) and analyzed with BD FACSDiva software (BD Biosciences). Nonspecific binding of reporter antibodies through Fc receptors was gated out before analysis. Binding is reported as mean fluorescence intensity.

Growth inhibition

Human Ramos Burkitt's lymphoma cells were obtained from the American Type Culture Collection and maintained in RPMI-1640 supplemented with HEPES and 10% heat-inactivated FBS at 37°C, 5% CO_2 unless otherwise stated. Ramos cells used in experiments were

between five and 30 passages. For effector-independent ATP assays, Ramos cells were seeded into a 96-well, flat-bottom white opaque microtiter plate (2×10^4 cells/0.1 ml) and incubated for 1 h before treatment with 1, 5, 10, or 25 μg/ml Rituxan or DXL625 as indicated or an equivalent volume of sterile SCS buffer. At the endpoint, the ATP-based luminescent CellTiter-Glo Reagent was prepared according to the manufacturer's instructions and added 1 : 1 (v/v) with cells. The plates were protected from light and incubated on an orbital shaker (1 h, room temperature) before luminescence reading by the Synergy 2 Multi-Mode Microplate Reader (Biotek, Winooski, Vermont, USA) and Gen5 Data Analysis Software (Biotek). Values for drug-treated cells were normalized to those measured for cells treated with saline and are reported as a fraction of luminescence.

Apoptosis, lipid-raft depletion, and calcium chelation

Apoptosis of Ramos cells were determined by quantifying the fraction of hypo-diploid cells (sub-G_0/G_1 DNA content) as identified by PI staining and separately confirmed by staining of activated capases with CaspACE reagent. For PI staining, Ramos cells were seeded (1.5×10^6 cells/5 ml) in a six-well format and incubated overnight. The cells were then treated with 1, 5, 10, or 25 μg/ml drug or an equivalent volume of sterile SCS buffer for 24 h. For processing, cells were washed twice with ice-cold phosphate buffered saline (PBS), fixed with ice-cold 95% ethanol (1 h, 4°C), washed twice again with ice-cold PBS, treated with 10 mg/ml RNase A (15 min, 37°C), stained with 1 mg/ml PI (15 min, room temperature), and acquired by flow cytometry. The cells were first gated by forward scatter-height (FSC-H) and forward scatter-width parameters to identify the total viable and nonviable populations and exclude noncellular debris. From the total cellular population, apoptotic cells were determined by measuring the percentage of sub-G_0/G_1 cells. Confirmatory labeling with FITC-conjugated CaspACE reagent (20 μmol/l/dimethyl sulfoxide) was done according to the manufacturer's instructions. Briefly, Ramos cells were seeded and treated with drug as above (24 h), washed once with PBS, stained with CaspACE (25 min, 37°C, 5% CO_2) on a shaker platform, washed again with PBS, and the mean fluorescence intensity and relative cellular population expressing active caspases were assessed by flow cytometry. For lipid raft depletion experiments, the maximal non-toxic concentration of MβCD for Ramos cells was determined by dose-limiting study and found to be 1% (w/v). Ramos cells were resuspended in media containing 1% MβCD for 1 h, washed and resuspended in fresh culture media, and treated with DXL625 or sterile SCS buffer equivalent (10 μg/ml, 24 h). Apoptotic cells were identified using the PI staining assay, using the procedure described above. For calcium chelation experiments, Ramos cells were resuspended in media supplemented with 10 mmol/l EDTA, followed by drug treatment and analysis by PI staining as above.

Complement-dependent cytotoxicity

CDC was assessed for drug-treated Ramos cells or primary B-lymphocytes from healthy donors. Ramos cells were seeded (2.5×10^5 cells/0.5 ml) in a 24-well format and incubated overnight. Next, 5% (v/v) rabbit HLA-ABC complement sera were added to cell cultures for 30 min before the addition of either Rituxan or DXL625 (10 μg/ml) or equivalent sterile SCS buffer. Rabbit complement sera were used instead of a human-derived complement to avoid complement inhibitory factors that could obscure results when comparing CDC induction. Following a 2-h drug incubation, viable and necrotic Ramos cells were stained with Calcein-AM and PI, respectively, and quantified by flow cytometry. Separately, frozen human PBLs were rapidly thawed and resuspended in complete media in a 24-well format (2.5×10^5 cells/0.5 ml) for 2 h before the addition of 5% (v/v) rabbit HLA-ABC complement sera. After 30 min, antibodies were added and allowed 2 h of incubation, at which point the proportion of B cells was determined by flow cytometry using PE-conjugated mouse anti-human CD19 antibodies. The whole lymphocyte population was first determined by FSC and SSC gating, where the decrease in the percentage of $CD19^+$ cells within this population was used to determine the relative decrease in B lymphocytes. Separate controls for CDC induction included treatment with sterile SSC buffer, either antibody alone, complement alone, or dual treatment of antibody and complement.

Antibody-dependent cellular cytotoxicity

To assess drug-dependent, effector cell-mediated cytotoxicity, $CD56^+$ (NK) cells were purified by immunomagnetic separation from normal human PBMC samples. Frozen human PBMCs were rapidly thawed and resuspended in complete media, incubated with magnetically labeled anti-CD56 micro-beads, and purified over magnetic separation columns according to the manufacturer's instructions. Effector cell purity ($CD56^+/CD16^+$) was confirmed by flow cytometric immunoprofiling. NK cells were added to Ramos cells in a ratio of 6 : 1 (effector : target ratio) in the presence of either drug (10 μg/ml) or equivalent sterile SCS buffer. After a 24-h incubation period, viability was determined using the CellTiter-Glo assay as above. The ATP content of effector cells remained unchanged over the incubation period in the presence or absence of drug and was corrected for using separate control cells.

Statistical analyses

Statistical analyses were performed using GraphPad Prism V4.0 (GraphPad, San Diego, California, USA). Data sets were first evaluated for significant within-group differences (greater than two SD from mean) and outliers were excluded from subsequent comparative analyses. For all in-vitro assays, a two-way analysis of variance and Bonferroni post test were used for assessing differences between treatment groups. The criterion for significance between groups was set at P value of less than 0.05.

Results

DXL625 displays enhanced binding and prolonged dissociation from target compared with Rituxan

Therapeutic antibodies directed against cell surface targets such as CD20 require acceptable association kinetics to mediate cytolytic effects. Prolongation of association with CD20 antigen (decreased off-rate) may further potentiate therapeutic effects [36]. The association and dissociation profiles of the DXL625 to CD20 antigen were compared with those of Rituxan using SPR. In initial experiments, SPR sensorgrams were compared for increasingly sparse CD20 peptide-mimetic (antigen) concentrations to determine whether target antigen density impacted the self-binding of DXL625. Both antibodies were also evaluated for nonspecific sensor chip surface interactions, and neither DXL625 nor Rituxan was found to bind irrelevant control peptides or peptide-deficient surfaces (data not shown). No observable binding was detected with human IgG1 isotype or DXL-conjugated IgG1 serving as the negative control analyte. As shown in Fig. 1a, the association kinetic signature of Rituxan at fixed concentration did not vary as a function of antigen coating density. A distinct autophilic binding profile was seen for DXL625, in which nonsaturable binding (RU values continue to increase throughout the analyte injection period) and prolongation of off-rate (return of maximum RU to baseline) were observed. However, this distinction was only seen at the two higher antigen-coating densities and was not evident at the lowest coating density (100 RU). The improved nonsaturable binding kinetics of DXL625 therefore appears to require a threshold antigen density.

To determine whether the results for SPR reflect binding to cognate CD20 antigen on cells, we compared the binding of DXL625 and Rituxan using healthy donor human B cells. CD20-positive cells within a population of human PBLs were stained with either antibody and examined by flow cytometry (Fig. 1b). The binding maximum (B_{max}) is 5.4-fold greater for DXL625 than Rituxan, indicating that the nonsaturable kinetic profile observed in SPR experiments reflects what is observed in live cells. Importantly, the binding of DXL625 and Rituxan could be blocked by the addition of recombinant cognate antigen, revealing that the increased B_{max} is not because of a function of nonspecific binding of DXL625 (data not shown). Moreover, control experiments using a DXL-conjugated human IgG1 isotype control showed no significant binding above the background (data not shown).

DXL625 displays enhanced effector-independent potency

Therapeutic anti-CD20 antibodies work through a combination of effector-dependent (Fc-mediated) and effector-independent (target-ligand-mediated) mechanisms. We assessed whether the increased B_{max} and prolonged off-rate of DXL625 would translate into enhanced effector-independent potency, CDC, or ADCC induction. To compare effector-independent potency, drug-induced effects of DXL625 were compared using as a target, the Ramos Burkitt's lymphoma cell line. ATP content, a generally acceptable measure of cellular viability and proliferation, was used to monitor antibody effects. Treatment of Ramos cells with either Rituxan or DXL625 elicited dose-dependent and time-dependent reduction in total cellular ATP content (Fig. 2a, b). At 24-h treatment duration, increasing concentrations of DXL625 (1, 5, 10, and 25 μg/ml) reduced ATP content by 18.4, 26.4, 29.7, and 31.1%, respectively, from control treated cells. These were statistically significant ($P < 0.05$, two-way analysis of variance) at all concentrations and significance was maintained in cells treated for 48 h. Comparison of DXL625 activity to that of Rituxan indicated significant reduction in ATP content (normalized to vehicle-treated cells) in the DXL625-treated cells. At 24 h, the relative reduction in ATP content between DXL625 and Rituxan were 81.6 versus 97.6, 73.6 versus 93.8, 70.3 versus 89.8, and 68.9 versus 88.5% ($P < 0.01$ for each concentration pairing) (Fig. 2a) and at 48 h 63.5 versus 83.4, 53.7 versus 84.4, 51.7 versus 75.3, and 51.5 versus 69.1% ($P < 0.01$ for each concentration, respectively) (Fig. 2b). Next, to determine whether any synergistic activities exist between DXL625 and Rituxan when coadministered to Ramos cells, standard addition experiments were performed. As the concentration of Rituxan in the culture media is reduced by 10% intervals from 10 to 0 μg/ml concentration and replaced on a molar basis with DXL625, the enhanced Fc-independent effect is restored at approximately 60% DXL625 : 40% Rituxan (Fig. 3). There are no apparent synergies observed between the two anti-CD20 antibodies. It is concluded from these data that reductions seen in total ATP content of treated cells might occur as a result of either reduced proliferation (metabolic rate), reduced viability (induction of cell death), or a combination of the two. Increasing concentrations of Rituxan decrease the fraction of receptor available for DXL625, supporting the idea of a minimum threshold density required for enhanced effector-independent potency seen with DXL625.

Enhanced effector-independent potency of DXL625 is because of apoptosis induction

Reduction of ATP content resulting from treatment with anti-CD20 antibodies could be a result of effects on proliferative rate, loss of viability, or a combination thereof. Rituxan has been reported to slow cell growth with no distinguishable arrest of cell cycle [37,38]. Furthermore, Rituxan monomers have been reported to trigger caspase-mediated, lipid raft-dependent apoptosis when a secondary anti-human IgG1 Fc-crosslinking antibody is added to the cells in culture [23,26,27]. PI staining and flow cytometric analysis of drug-treated Ramos cells was used to dually determine whether our

Fig. 1

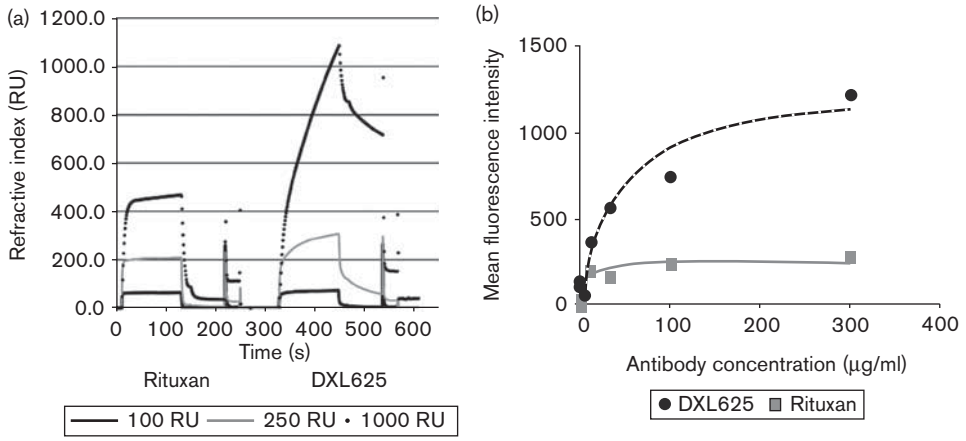

DXL625 displays prolonged dissociation rate from antigen and increased binding maximum compared with Rituxan. (a) Surface plasmon resonance (SPR) was used to compare the binding and dissociation kinetics of Rituxan and DXL625 with varying antigen densities, in which biotinylated CD20 peptide mimetic was immobilized to a streptavidin-coated sensor chip at three densities [increasing response units (RUs) correspond to greater immobilized antigen]. Rituxan or DXL625 (15 μg/ml) was flowed over the chip (120 s mAb/buffer for association, 60 s buffer for dissociation, 30 s acidic glycine for regeneration) and resulting change in relative RUs was compared. At 100 RU (lowest antigen density), saturable binding and rapid dissociation are similarly observed for Rituxan and DXL625, but nonsaturable binding and slowed dissociation from antigen are observed for DXL625 at higher densities. (b) Healthy donor peripheral blood lymphocyte samples were treated with varying concentrations of Rituxan and DXL625 (0–300 μg/ml). Binding for Rituxan is saturated at approximately 10 μg/ml, whereas specific binding of DXL625 continues to increase with higher concentrations. DXL625 displays a 5.4-fold increase in binding maximum compared with Rituxan.

Fig. 2

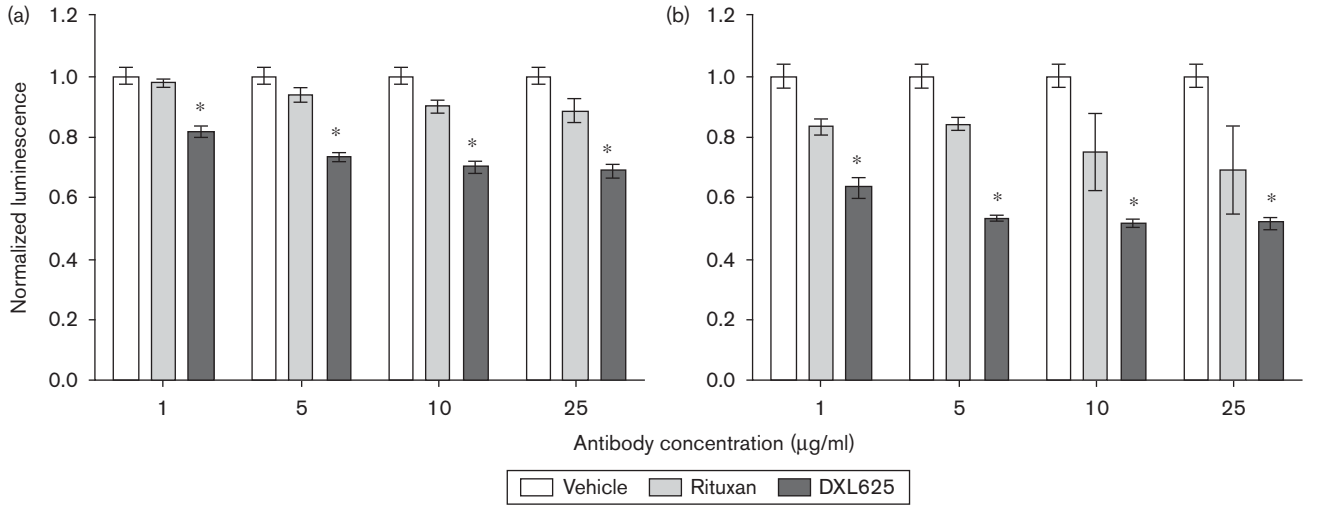

DXL625 and Rituxan treatment reduces total ATP content of Ramos cells. (a) After the indicated 24 h treatment (1, 5, 10, 25 μg/ml), the ATP content (measured by luminescence) for drug-treated cells was reported as fraction normalized to those buffer-treated (mean ± SD, $n=3$, $^*P<0.01$ DXL625 vs. Rituxan). (b) Relative reduction in cellular ATP is amplified with 48 h of drug treatment.

earlier observations were because of cell killing or reduction in proliferation. After 24-h exposure to DXL625, a significant increase in the proportion of sub-G_0/G_1 Ramos cells present in the pre-gated (live and non-viable) population was observed compared to Rituxan-treated or buffer-treated cells. Of note, the sub-G_0/G_1 cells induced by DXL625 were smaller in size (reduced FSC) and denser (increased SSC) (data not shown), supporting morphological progression through apoptosis. To further characterize loss of viability, treated cells were evaluated for the activation of caspases using a fluorescent pan-caspase substrate analog. DXL625 treatment (10 μg/ml)

Fig. 3

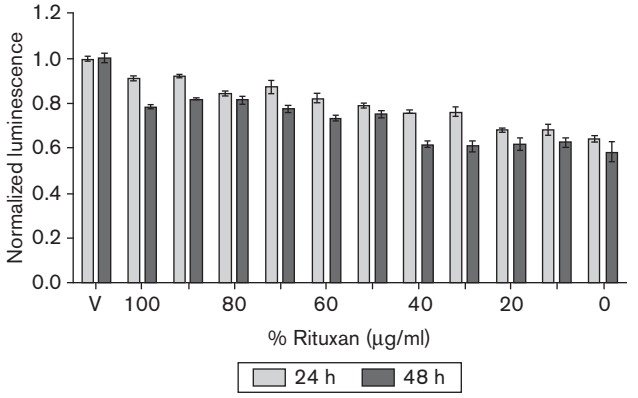

Treatment with an admixture of DXL625 and Rituxan reduces total ATP content of Ramos cells. The concentration of Rituxan (10 μg/ml) was reduced at 10% intervals and replaced by an equivalent molar amount of DXL625. Total cellular ATP content was assayed at 24 and 48 h of treatment and normalized to vehicle (v) treated cells. The enhanced Fc-independent effect is restored at approximately 60% DXL625: 40% Rituxan at 48 h with no apparent synergies between the two antibodies.

of Ramos cells resulted in a doubling of apoptotic events compared with equivalent Rituxan treatment (24.2 vs. 10.9%; $P < 0.05$). Moreover, caspase-positive cells possessed similar morphology as those in the sub-G_0/G_1 gate, confirming that these cells were indeed undergoing caspase-mediated apoptotic cell death (Fig. 4b–e). Thus, DXL625-mediated induction of apoptosis underlies, at least in part, the depletion of cellular ATP observed earlier.

DXL625-induced apoptosis selectively affects actively proliferating Ramos cells

In-vitro exposure of Ramos cells to DXL625 resulted in a reduction of cellular ATP because of the induction of apoptosis. As the cellular proliferation profile could also be affected by either antibody, treated cells were stained with PI and the proportions of cells in various stages of cell division (G_0/G_1, S-phase, and G_2/M) were analyzed by flow cytometry. Ramos cells treated with DXL625 showed a decrease in the fraction of S-phase cells (36.6, 29.7, 27.8, and 25.9% for 1, 5, 10, and 25 μg/ml, respectively) that correlated to increased apoptosis induction (9.5, 21.0, 24.9, and 30.0%), indicating that actively dividing cells were most susceptible to DXL625-induced apoptosis. Of note, when only viable cells were considered, no significant change in the proportion of cells in S-phase, G_0/G_1, or G_2/M was observed with increasing concentrations with DXL625. Furthermore, no significant change was seen between these phases with identical treatment with Rituxan, DXL625, or saline buffer (data not shown). These data suggest that (i) the cellular ATP reduction seen with DXL625 treatment is not because of altered proliferative activity in nonapoptotic cells, and (ii) actively dividing (S-phase) cells are most susceptible to DXL625-induced apoptosis.

DXL625-mediated apoptosis is lipid raft-dependent and is abrogated by calcium chelation

Rituxan has been reported to induce apoptosis in the presence of a cross-linking secondary antibody, purportedly through cholesterol-rich lipid raft signaling domains. To determine whether lipid raft integrity is required for the induction of apoptosis by DXL625, cholesterol was depleted from Ramos cell membranes before antibody exposure and analysis. To avoid the potential cytotoxic effects of MβCD while still ensuring adequate lipid raft dissolution, the highest concentration of MβCD that had no discernible effects on morphology, as determined by flow cytometry (FSC, SSC) and light microscopy, and DNA fragmentation (sub-G_0/G_1 cells) was used (1.0%). After MβCD or saline pretreatment, Ramos cells were treated for 24 h with DXL625 (10 μg/ml) and the fraction of cells undergoing apoptosis was assessed by PI staining and flow cytometry. The percentage of apoptotic cells treated with MβCD before DXL625 was significantly reduced compared with cells not treated with MβCD (10.6 ± 3.4 vs. $30.0 \pm 1.8\%$, $P = 0.036$), confirming the requirement for lipid raft integrity in DXL625-mediated apoptosis (Fig. 5a). As the CD20 receptor has been shown to be involved in the cellular influx of calcium, the proapoptotic effects of DXL625 were challenged by the addition of the chelator EDTA [27,39,40]. Prechelation of calcium from the cell culture media followed by the addition of DXL625 resulted in an abrogation of the proapoptotic effects of this autophilic anti-CD20 antibody (Fig. 5b). These experiments illustrate that the Fc-independent induction of apoptosis observed with DXL625 treatment requires cholesterol-enriched membrane fractions (lipid rafts) and calcium influx from extracellular pools.

DXL625 retains the Fc-dependent functions of Rituxan

Having established that DXL625 induces substantially greater levels of apoptosis than Rituxan, next we compared the abilities of DXL625 and Rituxan to induce CDC and NK cell-mediated ADCC in Ramos cells and primary B-lymphocytes from healthy donor PBLs. First, the ability of DXL625 to kill Ramos cells by complement fixation was tested. Flow cytometric analysis of treated Ramos cells revealed little change in the percentage of dead cells (PI staining) after 2-h incubation with DXL625 in the absence of complement, Rituxan in the absence of complement, or complement in the absence of the drug. The addition of complement in the presence of DXL625 or Rituxan resulted in significant cell killing (56.5 ± 1.1 or $48.6 \pm 2.8\%$, respectively, $P = 0.0023$) (Fig. 6a, left panel). Next, complement-mediated depletion of primary B-lymphocytes ($CD19^+$) was compared for DXL625 and Rituxan. Compared with incubation for 2 h with complement in the absence of the drug, DXL625 or Rituxan treatment in the absence of complement resulted in the depletion of $CD19^+$ lymphocytes ($23.4 \pm 1.6\%$ of lymphocyte gate vs. 12.6 ± 0.5 or $13.1 \pm 0.8\%$,

Fig. 4

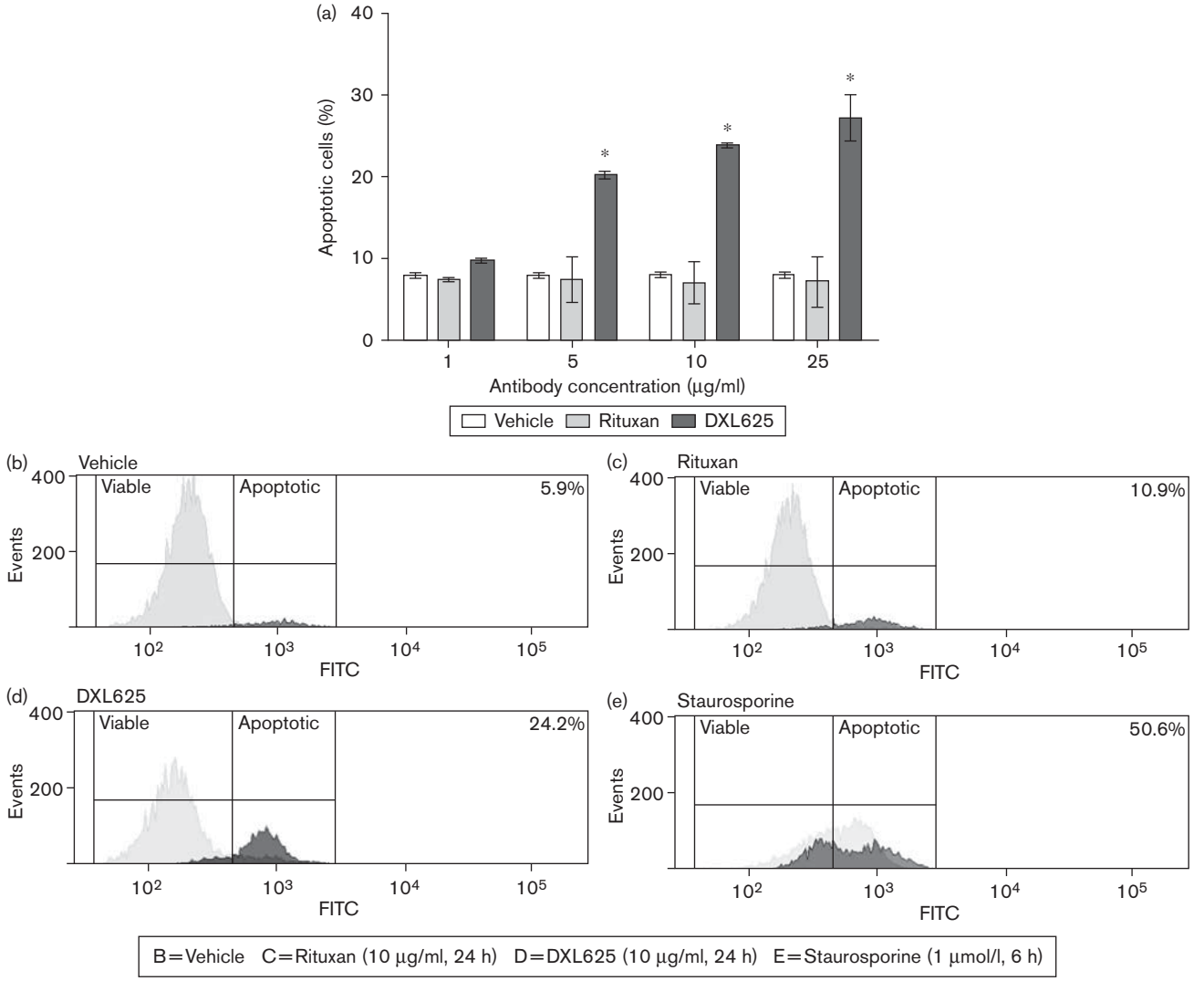

DXL625 induces caspase-mediated apoptosis. (a) Apoptosis induction in Ramos cells was first identified by a characteristic population of shrunken, hypodiploid (sub-G_0/G_1) cells, as analyzed by propidium iodide staining and flow cytometry. DXL625-induced significant levels of apoptosis in a dose-dependent manner whereas Rituxan did not (*$P<0.05$ DXL625 vs. Rituxan). Values are expressed as absolute percentages (mean ± SD, $n=3$) of the total cell population. (b–e) After drug treatment (10 μg/ml, 24 h), Ramos cells were stained for activated caspases and analyzed by flow cytometry. The percentages of caspase-positive cells are indicated (upper right-hand corner) for representative fluorescence histograms. Staurosporine (1 μmol/l, 6 h) served as a positive control for apoptosis induction in both experiments.

respectively). The reduction observed with antibody treatment in the absence of complement is suspected to be because of residual NK cells within the PBL population. Treatment with DXL625 or Rituxan plus complement resulted in further depletion of the $CD19^+$ lymphocyte population (3.1 ± 0.2 or 2.8 ± 0.4, respectively, $P = \text{NS}$) confirming that complement fixation indeed occurs with DXL625 (Fig. 6a, right panel). Next, we assessed the ability of DXL625 to induce NK cell-mediated ADCC in Ramos cells. Ramos cells were incubated with $CD56^+/CD16^+$ NK cells for 24 h in the presence or absence of 10 μg/ml DXL625 or Rituxan. Both DXL625 and Rituxan significantly reduced Ramos cell viability in the presence of NK cells when normalized to vehicle treatment (0.56 ± 0.05 and 0.77 ± 0.02, respectively, $P < 0.001$ for both) (Fig. 6b). Greater loss in target cell viability was seen for DXL625 than Rituxan in the presence or absence of NK cells ($P < 0.01$). However, the difference in viability seen with Rituxan in the presence or absence of NK cells was greater than that for DXL625, suggesting that (i) caspase-mediated apoptosis induced by DXL625 treatment alone may overlap pathways elicited by NK cell-released granzymes targeting Rituxan-opsonized cells or (ii) Fc-FcR interactions may result in sufficient antigen cross-linking for apoptosis induction already seen with DXL625 in the

Fig. 5

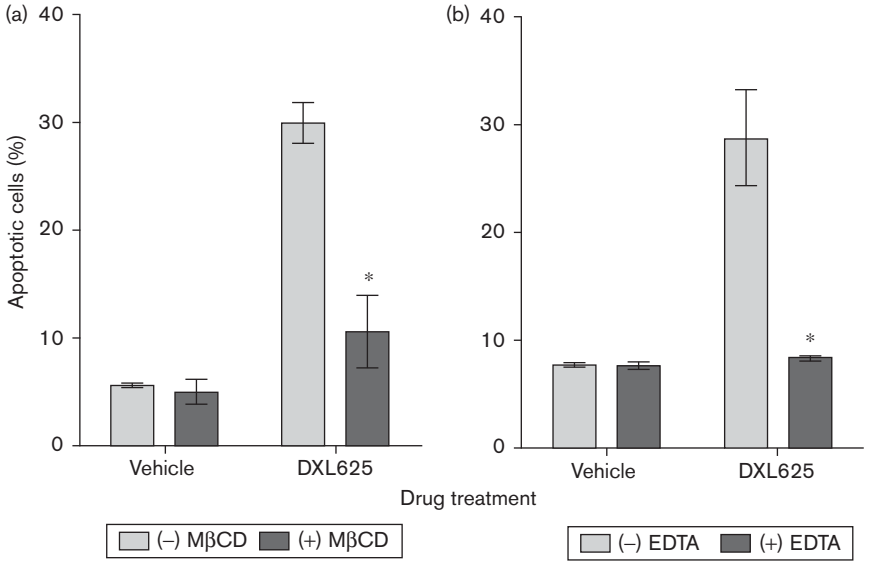

Induction of apoptosis by DXL625 requires lipid rafts and extracellular calcium. (a) Ramos cells were incubated with methyl-β-cyclodextran (MβCD) (1% w/v, 1 h) before being resuspended in fresh media and treated with DXL625 (10 μg/ml, 24 h). MβCD pretreatment significantly reduced DXL625-induced apoptosis as assessed by propidium iodide staining and flow cytometry (mean ± SD, $n=3$, $^*P<0.05$ DXL625 vs. MβCD + DXL625). (b) Ramos cells were resuspended in media containing 10-mmol/l EDTA and treated with DXL625 (10 μg/ml, 24 h). EDTA treatment significantly abrogated DXL625-induced apoptosis, as measured in a (mean ± SD, $n=3$, $^*P<0.05$ DXL625 vs. EDTA + DXL625).

absence of accessory cells. These data collectively show that DXL625 maintains the ability to fix complement and engage effector cells *in vitro*.

Discussion

In this study, we characterize the functional mechanisms of a novel therapeutic anti-CD20 antibody, DXL625, derived by ultraviolet photo-conjugation of an autophilic DXL peptide to Rituxan, a mouse/human chimeric IgGκ1 anti-CD20. DXL625 was designed to bind its antigenic target with greater avidity and with a prolonged dissociation rate compared with its parental antibody. We show here that DXL625 has (i) improved binding kinetics compared with Rituxan (prolonged off-rate, increased B_{max}), (ii) is endowed with autophilic binding properties (antigen-dependent antibody interassociation), (iii) exhibits markedly improved Fc-independent effects against the Ramos Burkitt's lymphoma cell line, (iv) induces caspase-mediated, lipid raft-dependent apoptosis, and (v) retains Fc-mediated CDC and ADCC immune effector responses.

The Fc-independent functions of Rituxan, while significant, are not completely defined and have since been proposed to include apoptosis induction and slowing of proliferation [12,37,38,41]. The induction of tumor cell apoptosis is controversial but has been clarified by recent reports [11,21–24,42,43]. Rituxan has long been presumed to induce apoptosis in malignant B cells *in vivo*, although evidence from patients is limited and does not preclude synergistic immune effects leading to caspase-mediated apoptosis [11,41]. For example, binding of Rituxan-opsonized cells by NK cells may result in apoptosis through (i) crosslinking of CD20 through multiple Fc-FcR engagements and (ii) granzyme release. In the absence of crosslinking reagents, Rituxan has been shown to not significantly induce apoptosis in established lymphoma cell lines *in vitro*, although it is crucial for sensitizing cells to chemotherapeutic drug-induced apoptosis, in part through downregulation of antiapoptotic proteins (Bcl-2, Bcl-xL, Mcl-1) and deactivation of constitutively activated cell survival pathways (PI3K-Akt, MEK-ERK1/2) [37,38,44–50]. This sensitizing effect is crucial for alleviating the patient's exposure to broad-spectrum, proapoptotic drugs such as doxorubicin while still yielding a beneficial effect. Therefore, it is reasonable to anticipate that anti-CD20 immunotherapeutic efficacy could be improved by 'engineering-in' autophilic binding properties with the goal of enhancing direct induction of cell death and thereby reducing the patient's exposure to toxic chemotherapeutic agents.

We have found that treatment of lymphoma cells with DXL625 resulted in dose-dependent and time-dependent formation of a subpopulation of cells morphologically consistent with an apoptotic phenotype (smaller/denser, sub-G_0/G_1 DNA content, and activated caspases). This effect was not seen with similar treatment with Rituxan. Experiments here show that enhanced binding to CD20-coated SPR sensor chips by DXL625 can be abrogated by limiting the antigen coating density,

Fig. 6

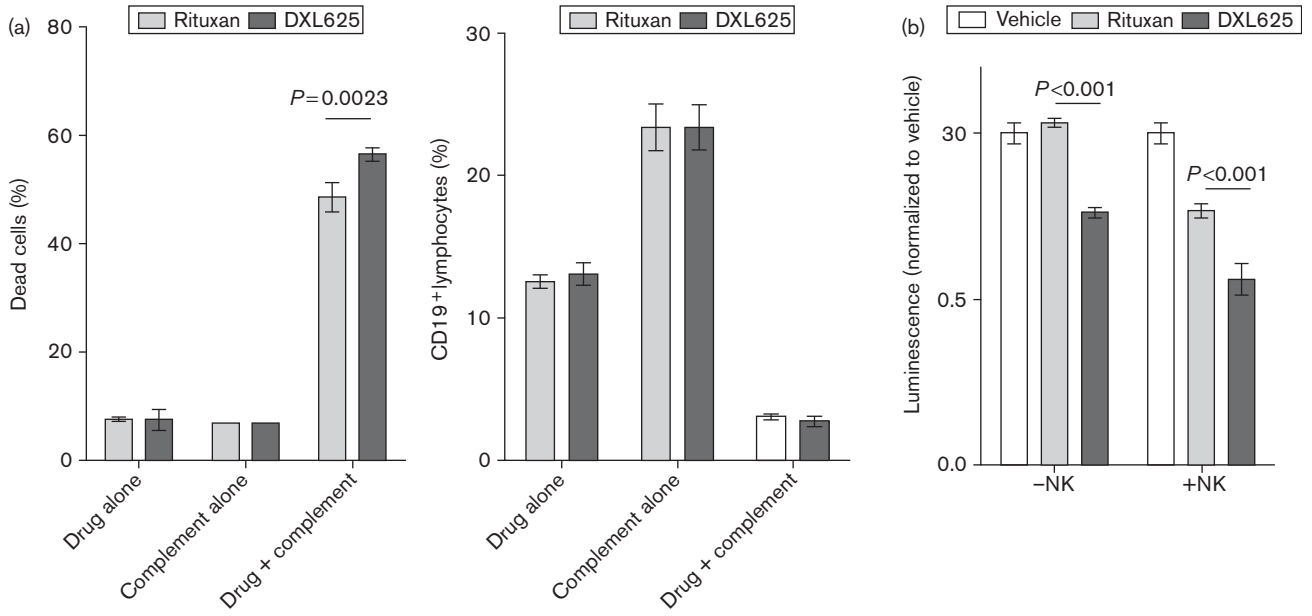

The Fc-dependent complement-dependent cytotoxicity (CDC) and antibody-dependent cellular cytotoxicity functions of Rituxan are maintained by DXL625. (a) (Left panel) CDC-induced Ramos cell death was assessed by propidium iodide staining of Rituxan and DXL625-treated cells (10 μg/ml, 2 h) in the presence or absence of complement sera (5% v/v, 30 min). Cells were analyzed by flow cytometry and values reported as absolute percentages (mean ± SD, $n=3$). In the presence of complement, DXL625-induced significantly greater Ramos cell death than Rituxan ($P=0.0023$). (Right panel) CDC was assessed for peripheral blood lymphocytes samples using flow cytometry as described in the Methods section. Both DXL625 and Rituxan treatment resulted in a decrease in the proportion of $CD19^+$ lymphocytes when supplemented with complement (mean ± SD, $n=2$). (b) Effector cell-mediated killing is enhanced by DXL625. Ramos cells were treated with purified natural killer (NK) cells (6 : 1 effector : target) in the presence or absence of drug (10 μg/ml, 24 h) and changes in cellular ATP were measured as described in the Methods section. Values are reported as a fraction of luminescence of NK-treated cells in the absence of drug (mean ± SD, $n=3$). Significantly greater NK cell-mediated killing is seen with DXL625 compared with Rituxan ($P<0.001$).

suggesting that the characteristic antibody interassociation by DXL625 requires some antigen density threshold. Drug-induced translocation of CD20 receptor molecules to lipid raft microenvironment may transiently result in localized regions of high CD20 density, reflecting the prolonged dissociation kinetics seen with higher CD20 sensor chip densities. Earlier work by Unruh *et al.* and Janas *et al.* [26,27] indicated that the propoptotic effect of Rituxan observed in the presence of a cross-linking secondary antibody had the requirement for lipid rafts and a source for calcium influx, and pretreatment with MβCD or a calcium-chelating agent abolished the effect. Present data suggest a requirement for lipid raft integrity and for an extracellular source of calcium in potentiating DXL625-induced apoptosis.

Importantly, we show that despite being altered by conjugation to DXL peptide, DXL625 retains the Fc-mediated CDC and ADCC functions of Rituxan. The failure of Rituxan therapy in certain patients is more clearly explained by variations in Fc γ-receptor genotypes and impaired ADCC activation rather than factors affecting complement [12,29–31]. This lends support to the idea that engagement of Rituxan-opsonized target cells by FcR-expressing cells, at least in these patients, is more important for tumor clearance than any direct cytolytic or complement-mediated effects by Rituxan in the absence of effector cell binding. Given the potential role of NK cell-mediated ADCC in inducing target cell apoptosis, either by the release of caspase-activating granzymes or crosslinking of CD20 surface molecules through Fc-FcR interactions, the pro-apoptotic effects observed with DXL625 may prove beneficial for patients, particularly for those whose lack of response to Rituxan is linked to FcR genotypic variation. Although determining the relative importance for each mode of action of Rituxan has only been possible thus far by grouping patients who have not responded to therapy, it may be possible to confirm the mechanisms for DXL625 by which added therapeutic benefit is achieved in future in-vivo studies.

In conclusion, we report that the autophilic anti-CD20 antibody, DXL625, is unique in its ability to mediate Fc-independent apoptosis without the need for a crosslinking secondary antibody. Modification through conjugation to the autophilic DXL peptide did not impair Fc-mediated effector functions and as such makes this therapeutic candidate particularly attractive for development for use in B-cell lymphoma patients unresponsive to Rituxan.

Acknowledgements

Disclosure statements: (i) The study sponsor had no role in the interpretation of data and had no influence in the writing of this report or the decision to submit the report for publication. (ii) Marc G. Bingaman and Thomas J. Kindt are employed by InNexus Biotechnology (Scottsdale, AZ). Gargi D. Basu and Tiana C. Golding are now employed by Caris Life Sciences (Phoenix, AZ). Samuel K. Chong is now employed by Genentech (San Francisco, CA). Marc G. Bingaman wrote the manuscript and designed and performed experiments. Gargi D. Basu, Tiana C. Golding, Samuel K. Chong, and Andrew J. Lassen designed and performed experiments. Thomas J. Kindt and Christopher A. Lipinski designed experiments and wrote the manuscript. Industry support: InNexus Biotechnology, Inc. funded and supplied materials of studies.

References

1 Von Mehren M, Adams GP, Weiner LM. Monoclonal antibody therapy for cancer. *Annu Rev Med* 2003; **54**:343–369.
2 Campbell P, Marcus R. Monoclonal antibody therapy for lymphoma. *Blood Rev* 2003; **17**:143–152.
3 Hale G. Therapeutic antibodies – delivering the promise? *Adv Drug Deliv Rev* 2006; **7**:633–639.
4 Scallon BJ, Snyder LA, Anderson GM, Chen Q, Yan L, Weiner LM, *et al.* A review of antibody therapeutics and antibody-related technologies for oncology. *J Immunother* 2006; **29**:351–364.
5 Fleischmann RM. Safety of biologic therapy in rheumatoid arthritis and other autoimmune diseases: focus on rituximab. *Semin Arthritis Rheum* 2009; **38**:265–280.
6 Davis TA, Grillo-López AJ, White CA, McLaughlin P, Czuczman MS, Link BK, *et al.* Rituximab anti-CD20 monoclonal antibody therapy in non-Hodgkin's lymphoma: safety and efficacy of re-treatment. *J Clin Oncol* 2000; **18**:3135–3143.
7 Plosker GL, Figgitt DP. Rituximab: a review of its use in non-Hodgkin's lymphoma and chronic lymphocytic leukemia. *Drugs* 2003; **63**:803–843.
8 Boye J, Elter T, Engert A. An overview of the current clinical use of the anti-CD20 monoclonal antibody rituximab. *Ann Oncol* 2003; **14**:520–535.
9 Robak T. Novel monoclonal antibodies for the treatment of chronic lymphocytic leukemia. *Curr Cancer Drug Targets* 2008; **8**:156–171.
10 Kim JJ, Thrasher AJ, Jones AM, Davies EG, Cale CM. Rituximab for the treatment of autoimmune cytopenias in children with immune deficiency. *Br J Haematol* 2007; **138**:94–96.
11 Eisenbeis CF, Caligiuri MA, Byrd JC. Rituximab: converging mechanisms of action in non-Hodgkin's lymphoma? *Clin Cancer Res* 2003; **9**:5810–5812.
12 Maloney DG, Smith B, Rose A. Rituximab: mechanism of action and resistance. *Semin Oncol* 2002; **29**:2–9.
13 Smith MR. Rituximab (monoclonal anti-CD20 antibody): mechanisms of action and resistance. *Oncogene* 2003; **22**:7359–7368.
14 Cragg MS, Bayne MC, Illidge TM, Valerius T, Johnson PW, Glennie MJ. Apparent modulation of CD20 by rituximab: an alternative explanation. *Blood* 2004; **103**:3989–3990.
15 Glennie MJ, French RR, Cragg MS, Taylor RP. Mechanisms of killing by anti-CD20 monoclonal antibodies. *Mol Immunol* 2007; **44**:3823–3837.
16 Clynes RA, Towers TL, Presta LG, Ravetch JV. Inhibitory Fc receptors modulate *in vivo* cytotoxicity against tumor targets. *Nat Med* 2000; **6**:443–446.
17 Di Gaetano N, Cittera E, Nota R, Vecchi A, Grieco V, Scanziani E, *et al.* Complement activation determines the therapeutic activity of rituximab *in vivo*. *J Immunol* 2003; **171**:1581–1587.
18 Cragg MS, Glennie MJ. Antibody specificity controls *in vivo* effector mechanisms of anti-CD20 reagents. *Blood* 2004; **103**:2738–2743.
19 Golay J, Manganini M, Facchinetti V, Gramigna R, Broady R, Borleri G, *et al.* Rituximab-mediated antibody-dependent cellular cytotoxicity against neoplastic B cells is stimulated strongly by interleukin-2. *Haematologica* 2003; **88**:1002–1012.
20 Golay J, Cittera E, Di Gaetano N, Manganini M, Mosca M, Nebuloni M, *et al.* The role of complement in the therapeutic activity of rituximab in a murine B lymphoma model homing in lymph nodes. *Haematologica* 2006; **91**:176–183.
21 Ghetie MA, Bright H, Vitetta ES. Homodimers but not monomers of Rituximab (chimeric anti-CD20) induce apopotosis in human B-lymphoma cells and synergize with a chemotherapeutic agent and an immunotoxin. *Blood* 2001; **97**:1392–1398.
22 Pedersen IM, Buhl AM, Klausen P, Geilser CH, Jurlander J. The chimeric anti-CD20 antibody rituximab induces apoptosis in B-cell chronic lymphocytic leukemia cells through a p38 mitogen activated protein-kinase-dependent mechanism. *Blood* 2002; **99**:1314–1319.
23 Van der Kolk LE, Evers LM, Omene C, Lens SM, Lederman S, van Lier RA, *et al.* CD20-induced B cell death can bypass mitocondria and caspase activation. *Leukemia* 2002; **16**:1735–1744.
24 Zhang N, Khawli LA, Hu P, Epstein AL. Generation of rituximab polymer may cause hyper-cross-linking-induced apoptosis in non-Hodgkin's lymphomas. *Clin Cancer Res* 2005; **11**:5971–5980.
25 Cardarelli PM, Quinn M, Buckman D, Fang Y, Colchr D, King DJ, *et al.* Binding to CD20 by anti-B1 antibody or F(ab')(2) is sufficient for induction of apoptosis in B-cell lines. *Cancer Immunol Immunother* 2002; **51**:15–24.
26 Unruh TL, Li H, Mutch CM, Shariat N, Grigoriou L, Sanyal R, *et al.* Cholesterol depletion inhibits src family kinase-dependent calcium mobilization and apoptosis induced by rituximab crosslinking. *Immunology* 2005; **16**:223–232.
27 Janas E, Priest R, Wilde JE, White JH, Malhotra R. Rituxan (anti-CD20 antibody)-induced translocation of CD20 into lipid rafts is crucial for calcium influx and apoptosis. *Clin Exp Immunol* 2005; **139**:439–446.
28 Stavenhagen JB, Gorlatov S, Tuaillon N, Rankin CT, Li H, Burke S, *et al.* Fc optimization of therapeutic antibodies enhance their ability to kill tumor cells *in vitro* and controls tumor expansion *in vivo* via low-affinity activating Fcgamma receptors. *Cancer Res* 2007; **67**:8882–8890.
29 Cartron G, Dacheux L, Salles G, Solal-Celigny P, Bardos P, Colombat P, *et al.* Therapeutic activity of humanized anti-CD20 monoclonal antibody and polymorphism in IgG Fc receptor FcgammaRIIIa gene. *Blood* 2002; **99**:754–758.
30 Weng WK, Levy R. Two immunoglobulin G fragment C receptor polymorphisms independently predict response to rituximab in patients with follicular lymphoma. *J Clin Oncol* 2003; **21**:3940–3947.
31 Dall'Ozoo S, Tartas S, Paintaud G, Cartron G, Colombat P, Bardos P, *et al.* Rituximab-dependent cytotoxicity by natural killer cells: influence of FCGR3A polymorphism on the concentration-effect relationship. *Cancer Res* 2004; **64**:4464–4469.
32 Zhao Y, Kohler H. Enhancing tumor targeting and apoptosis using noncovalent antibody homodimers. *J Immunother* 2002; **25**:396–404.
33 Zhao Y, Lou D, Burke J, Kohler H. Enhanced anti-B-cell tumor effects with anti-CD20 superantibody. *J Immunother* 2002; **25**:57–62.
34 Kaveri SV, Kang CY, Kohler H. Natural mouse and human antibodies bind to a peptide derived from a germline VH chain. Evidence for evolutionary conserved self-binding locus. *J Immunol* 1990; **145**:4207–4213.
35 Halpern R, Kaveri SV, Kohler H. Human anti-phosphorylcholine antibodies share idiotopes and are self-binding. *J Clin Invest* 1991; **88**:476–482.
36 Teeling JL, French RR, Cragg MS, van den Brakel J, Pluyter M, Huang H, *et al.* Characterization of new human CD20 monoclonal antibodies with potent cytolytic activity against non-Hodgkin lymphomas. *Blood* 2004; **104**:1793–1780.
37 Alas S, Emmanouilides C, Bonavida B. Inhibition of interleukin 10 by rituximab results in down-regulation of bcl-2 and sensitization of B-cell non-Hodgkin's lymphoma to apoptosis. *Clin Cancer Res* 2001; **7**:709–723.
38 Jazirehi AR, XH G, De Vos S, Emmanouilides C, Bonavida B. Rituximab (anti-CD20) selectively modified Bcl-xL and apoptosis protease activating factor-1 (Apaf-1) expression and sensitizes human non-Hodgkin's lymphoma B cell lines to paclitaxel-induced apoptosis. *Mol Cancer Ther* 2003; **2**:1183–1193.
39 Bubien JK, Zhou LJ, Bell PD, Frizzell RA, Tedder TF. Transfection of the CD20 cell surface molecule into ectopic cell types generates a Ca^{2+} conductance found constitutively in B lymphocytes. *J Cell Biol* 1993; **121**:1121–1132.
40 Hofmeister JK, Cooney D, Coggeshall KM. Clustered CD20 induced apoptosis: src-family kinase, the proximal regulator of tyrosine phosphorylation, calcium influx, and caspase 3-dependent apoptosis. *Blood Cells Mol Dis* 2000; **26**:133–143.
41 Byrd JC, Kitada S, Flinn IW, Aron JL, Pearson M, Lucas D, *et al.* The mechanism of tumor cell clearance by rituximab *in vivo* in patients with B-cell chronic lymphocytic leukemia: evidence of caspase activation and apoptosis induction. *Blood* 2002; **99**:1038–1043.

42 Deans JP, Li H, Polyak MJ. CD20-mediated apoptosis: signalling through lipid rafts. *Immunology* 2002; **107**:176–182.
43 Daniels I, Abulayha AM, Thomson BJ, Haynes AP. Caspase-independent killing of Burkitt lymphoma cell lines by rituximab. *Apoptosis* 2006; **11**:1013–1023.
44 Alas S, Bonavida B. Rituximab inactivates signal transducer and activation of transcription 3 (STAT3) activity in B-non-Hodgkin's lymphoma through inhibition of the interleukin 10 autocrine/paracrine loop and results in down-regulation of Bcl-2 and sensitization to cytotoxic drugs. *Cancer Res* 2001; **61**:5137–5144.
45 Bonavida B, Vega MI. Rituximab-mediated chemosensitization of AIDS and non-AIDS non-Hodgkin's lymphoma. *Drug Resist Updat* 2005; **8**:27–41.
46 Bonavida B. Rituximab-induced inhibition of antiapoptotic cell survival pathways: implications in chemo/immunoresistance, rituximab unresponsiveness, prognostic, and therapeutic interventions. *Oncogene* 2007; **26**:3629–3636.
47 Hussain SR, Cheney CM, Johnson AJ, Lin TS, Grever MR, Caligiuri MA, *et al.* Mcl-1 is a relevant therapeutic target in acute and chronic lymphoid malignancies: down-regulation enhances rituximab-mediated apoptosis and complement-mediated cytotoxicity. *Clin Cancer Res* 2007; **13**:2144–2150.
48 Jazirehi AR, Vega MI, Chatterjee D, Goodglick L, Bonavida B. Inhibition of the Raft-MEK1/2-ERK1/2 signaling pathway, Bcl-xL down-regulation, and chemosensitization of non-Hodgkin's lymphoma B cells by Rituximab. *Cancer Res* 2004; **64**:7117–7726.
49 Jazirehi AR, Bonavida B. Cellular and molecular signal transduction pathways modulated by rituximab (rituxan, anti-CD20 mAb) in non-Hodgkin's lymphoma: implications in chemosensitization and therapeutic intervention. *Oncogene* 2005; **24**:2121–2143.
50 Suzuki E, Umezawa K, Bonavida B. Rituximab inhibits the constitutively activated PI3K-Akt pathway in B-NHL cell lines: involvement in chemosensitization to drug-induced apoptosis. *Oncogene* 2007; **26**:6184–6193.